

See discussions, stats, and author profiles for this publication at: <https://www.researchgate.net/publication/263974739>

# Emergence and Amplification of Chirality via Achiral–Chiral Polymorphic Transformation in Sodium Chlorate Solution Growth

ARTICLE in CRYSTAL GROWTH & DESIGN · JUNE 2014

Impact Factor: 4.89 · DOI: 10.1021/cg500527t

---

CITATION

1

READS

83

## 8 AUTHORS, INCLUDING:



[Yuki Kimura](#)

Hokkaido University

151 PUBLICATIONS 705 CITATIONS

[SEE PROFILE](#)



[Shunta Harada](#)

Nagoya University

46 PUBLICATIONS 170 CITATIONS

[SEE PROFILE](#)



[Toru Ujihara](#)

Nagoya University

189 PUBLICATIONS 1,408 CITATIONS

[SEE PROFILE](#)

# Emergence and Amplification of Chirality via Achiral–Chiral Polymorphic Transformation in Sodium Chlorate Solution Growth

Hiromasa Niinomi,<sup>\*,†</sup> Hitoshi Miura,<sup>‡</sup> Yuki Kimura,<sup>§,⊥</sup> Makio Uwaha,<sup>||</sup> Hiroyasu Katsuno,<sup>†,@</sup> Shunta Harada,<sup>†</sup> Toru Ujihara,<sup>†</sup> and Katsu Tsukamoto<sup>§</sup>

<sup>†</sup>Department of Materials Science and Engineering, Graduate School of Engineering, Nagoya University, Furo-cho, Chikusa, Nagoya, Aichi 464-8603, Japan

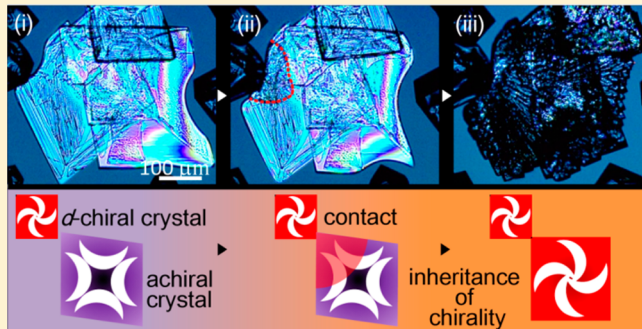
<sup>‡</sup>Graduate School of Natural Sciences, Nagoya City University, Yamanohata, Mizuho-cho, Mizuho, Nagoya, Aichi 467-8501, Japan

<sup>§</sup>Department of Earth and Planetary Materials Science, Graduate School of Science, Tohoku University, Aramaki, Aoba, Sendai, Miyagi 980-8578, Japan

<sup>||</sup>Department of Physics, Graduate School of Science, Nagoya University, Furo-cho, Chikusa, Nagoya, Aichi 464-860, Japan

## S Supporting Information

**ABSTRACT:** Chiral symmetry breaking during the chiral crystallization from a sodium chlorate ( $\text{NaClO}_3$ ) aqueous solution is an intriguing phenomenon because it provides insights into the prebiotic process of biohomochirality. However, a mechanism of the emergence and amplification of chirality remains controversial, especially for crystallization from highly supersaturated solution, and one of the hypotheses proposed before is a transition toward the homochiral state during the early stages of crystallization. In this contribution, we directly examined the early stage of crystallization by *in situ* polarized-light microscopy. The observation revealed that achiral crystals, which appear prior to the formation of chiral crystals, transform to the chiral crystal through two kinds of polymorphic transformations: (1) martensitic transformation (MT) and (2) solution-mediated phase transition (SMPT). The SMPT is remarkably facilitated by contact with a chiral crystal. Notably, the resulting enantiomorph through contact-facilitated SMPT is strongly directed by the contacting enantiomorph. In contrast, the MT yields two enantiomorphs in equal probability. The emergence and amplification of chirality has generally been considered to be a result of direct nucleation of a chiral crystal and its fragmentation. In contrast, our observations provide a possibility that the MT and contact-facilitated SMPT play a role for the emergence and amplification of chirality, respectively.



## INTRODUCTION

Chiral symmetry breaking in sodium chlorate ( $\text{NaClO}_3$ ) crystallization from agitated aqueous solutions<sup>1–8</sup> is an intriguing phenomenon because of the potential to provide insights into the prebiotic process of biohomochirality and practical methodologies for chiral separation. The emergence and amplification of chirality are often debated, especially when one considers the mechanism of chiral symmetry breaking. The crystallization of  $\text{NaClO}_3$  is a typical example of chiral crystallization. An achiral solution of  $\text{NaClO}_3$  yields chiral, enantiopure crystals with cubic  $P2_13$  enantiomorphous symmetry [Figure 1A (i)].<sup>9</sup> Since both the enantiomorphs are equally thermodynamically favorable, statistically equal numbers of the enantiomorphs are obtained via crystallization from a static solution.<sup>10</sup> However, it was discovered by Kondepudi et al.<sup>1</sup> that stirring during crystallization leads to a significant bias in the population of the two enantiomorphs (i.e., the emergence of a homochiral state). Since Kondepudi's discovery, many crystallization experiments have been carried out under various

modes of perturbation in order to investigate the underlying factors of the homochiral state.<sup>11–16</sup>

Crystallization experiments are roughly classified into two types according to whether or not primary nucleation is involved: (1) far-from-equilibrium involving primary nucleation processes<sup>1–5</sup> as represented by Kondepudi's experiment and (2) quasi-equilibrium seemingly irrelevant to primary nucleation, as represented by Viedma's demonstration whereby a racemic mixture in contact with a saturated solution converted to a homochiral state by stirring the aqueous suspension in the presence of glass beads.<sup>8</sup> Notably, in far-from-equilibrium experiments, homochiral states occur through the production of secondary crystals originating from the fragmentation of a single "mother crystal" that appeared during primary nucleation.<sup>1,11–13</sup> However, it is still arguable whether

Received: April 16, 2014

Revised: June 5, 2014

Published: June 5, 2014

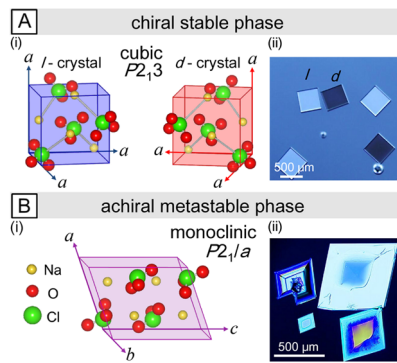


**Figure 1.** Polymorphism in  $\text{NaClO}_3$  crystallization from aqueous solution under normal pressure: (A) stable chiral cubic phase. (i) Crystal structure of the chiral cubic phase. (ii) Micrograph of the chiral cubic crystal captured by a polarized-light microscope (under noncrossed Nicols). (B) Metastable achiral monoclinic phase. (i) Crystal structure of the achiral monoclinic phase. (ii) Micrograph of the achiral monoclinic crystal captured by a polarized-light microscope (under crossed Nicols).

secondary crystals can explain the homochiral state in crystallizations from highly supersaturated solutions,<sup>3–5</sup> because a high rate of primary nucleation, which produces two enantiomorphs in equal probability, caused by supersaturation should lead to the absence of the specific “mother crystal” (Note: that the Viedma’s experiment in ref 5 is distinct from the Viedma’s experiment under quasi-equilibrium conditions). For this reason, a transition toward a homochiral state during the earliest stage of crystallization, the primary nucleation or precritical cluster stage, has been proposed.<sup>3–6,17</sup> Nevertheless, a direct observation of the actual events during the early stage was missing.

Recently, we carried out *in situ* microscopic observations of the early stage of crystallization using a droplet-evaporation method.<sup>18</sup> The observations revealed that an achiral monoclinic polymorph appeared prior to the formation of the chiral crystal (Figure 1B) and transformed to chiral crystals within a few minutes, while following Ostwald’s rule of stages. We also reported that the solubility of the achiral polymorph was about 1.6 times larger than that of the chiral crystal,<sup>19</sup> indicating that the crystallization process, initiated by the formation of the achiral crystal, possibly occurred from a highly supersaturated solution. Therefore, the achiral–chiral polymorphic transformation, which was not considered in previously proposed hypotheses on chiral symmetry breaking, has potential to provide novel insights into the homochiral state of crystallizations from highly supersaturated solutions.

The role of the transformation on the resulting handedness of the crystals still remains unclear because of a lack of detailed observations that focus on the transformation. Therefore, here we present detailed *in situ* observations with intensive attention to the achiral–chiral polymorphic transformation using polarized-light microscopy with a high-resolution video recording system. We demonstrate that two different kinds of polymorphic transformations have the potential to play roles in the spontaneous emergence and amplification of chirality.

## MATERIALS AND METHODS

**Solution Preparation.** A saturated aqueous solution of  $\text{NaClO}_3$  was prepared by dissolving  $\text{NaClO}_3$  powder of chiral cubic crystals (110 g; Analytical grade, Wako Pure Chemical

Industries, Ltd., Osaka) in ultrapure water (100 mL) in a glass beaker at room temperature ( $22^\circ\text{C}$ ). The  $\text{NaClO}_3$  powder was used as received. The resulting solution was then heated to  $30^\circ\text{C}$  with stirring via a magnetic hot plate. After assuring that the powder was completely dissolved in the water, the beaker was hermetically closed using laboratory film, and left for a week at the room temperature ( $22^\circ\text{C}$ ) to precipitate the solute dissolved in excess of the chiral cubic phase solubility. After the precipitation, the solution reached equilibrium at  $22^\circ\text{C}$ . The supernatant of the resulting solution was then used as a saturated solution for observations.

**Observation of Achiral–Chiral Polymorphic Transformation during Crystallization from an Aqueous Solution.** We observed the crystallization processes in a droplet of the prepared solution using a microscope. A polarized-light microscope [BX51-P (custom-made); Olympus Corp., Tokyo, Japan] and a high-resolution video system (HDTV) were employed because a polarized-light microscope can distinguish the handedness of enantiomorphs by detecting the difference in the direction of optical rotation. The difference can be easily detected by rotating an analyzer a few degrees from the crossed Nicols [Figure 1A (ii)].<sup>7</sup> Moreover, the microscope allowed us to distinguish cubic crystals from noncubic crystals because the latter has detecting optical birefringence but the former does not, that is, we could distinguish  $\text{NaClO}_3$  chiral crystals from  $\text{NaClO}_3$  achiral crystals *in situ* [Figure 1A (ii) and 1B (ii)]. The crystallizations were induced by evaporation of the droplet. The saturated solution (6  $\mu\text{L}$ ) was placed on a glass slide using a micropipet. The temperature of the glass slide was controlled at  $22^\circ\text{C}$  with an accuracy of  $\pm 0.1^\circ\text{C}$  using a thermostated stage with a Peltier element. Thus, the temperature was maintained at  $22^\circ\text{C}$  throughout the crystallization. After being placed on the glass slide, the droplet was left to evaporate. The evaporation increases the degree of supersaturation, inducing crystallization. After about 10 min, a few crystals appeared in the droplet. The crystallization process was captured using a high-definition (HD) recording system consisting of a video camera (SONY HDC-X300).

**Observation of Achiral–Chiral Polymorphic Transformation in Air.** In addition to the *in situ* observation of crystallization from an aqueous solution, we also examined transformations of crystals completely exposed to air. Namely, an achiral–chiral polymorphic transformation that did not involve solvent was observed. The crystal was prepared by the antisolvent crystallization method. The method using acetone was reported to be able to extract achiral crystals from the mother solution.<sup>19</sup> The solution prepared by the aforementioned procedure (see Solution Preparation) was used as the mother solution for the antisolvent crystallization. The mother solution was placed on a glass slide using a micropipet (6  $\mu\text{L}$ ), and then about 500  $\mu\text{L}$  of acetone was flushed into the mother solution. After flushing, the glass slide was dried by a dryer until the solvent was completely evaporated. The obtained achiral crystals were 50–100  $\mu\text{m}$  in size. After confirming the complete evaporation under the polarized-light microscope, we stimulated the achiral crystal at  $22^\circ\text{C}$  by touching the crystal with the tip of a needle while observing the crystal with a polarized-light microscope.

## RESULTS

**Observation of Achiral–Chiral Polymorphic Transformation in Crystallization from Aqueous Solution.**

Figure 2 shows time-lapse micrographs of the crystallization induced by droplet-evaporation. Bright crystals were initially

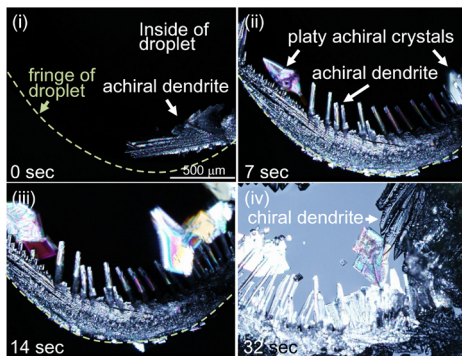


**Figure 2.** In situ polarized light microscopic images of  $\text{NaClO}_3$  crystallization induced by the droplet-evaporation method: (i) dendritic growth of achiral crystal after nucleation (under crossed Nicol); (ii) platy parallelogram-shaped achiral crystal, which appears in the vicinity of achiral dendrites (under crossed Nicol); (iii) achiral dendrites growing toward the center of the droplet (under crossed Nicol); and (iv) achiral dendrites transforming to the chiral phase and the appearance of chiral dendrites (under noncrossed Nicol).

formed near the meniscus of the droplet. The bright crystals were monoclinic crystals because noncubic crystals exhibit bright contrast under crossed Nicols owing to birefringence. The achiral crystals had a dendritic shape. The dendritic crystals grew preferentially along the fringe and maintained their dendritic shape (Figure 2i). Subsequently, platy parallelogram crystals appeared around the dendrites (Figure 2ii). The parallelogram crystals moved to the center of the droplet by induced flow as they grew to a size of less than 1 mm. On the other hand, the achiral dendrites continued to grow larger than 1 mm preferentially along the meniscus, and they simultaneously grew toward the center of the droplet (Figure 2iii). Several seconds after the formation of the achiral dendrites, the bright contrast of the achiral dendrites partially disappeared in the microscopic region where the dendrites initially formed. The disappearance of the bright contrast indicates that the achiral crystal transformed to a chiral cubic crystal with no birefringence. After the first extinction, the dark region began to spread along the achiral dendrites with a velocity of about 20  $\mu\text{m/sec}$  from the region where the transformation started (Figure 2iv). With time, the achiral dendrites were completely converted into chiral crystals. The resulting shape of the chiral crystals nearly retained the shape of the achiral dendrites, displaying a pseudomorph of the dendrites. After the conversion, the chiral dendrites continued to grow toward the center of the droplet. Consequently, the chiral dendrites approached the parallelogram platy achiral crystals.

The parallelogram achiral crystals showed two different types of behaviors, depending on the distance from the chiral dendrites (see video, cg500527t\_si\_002.avi, of the Supporting Information). First, when the chiral dendrites reached within 20  $\mu\text{m}$  of a parallelogram achiral crystal, the achiral crystal started to dissolve [Figure 3A (i)]. The achiral crystal continued to dissolve in response to the growth of the chiral dendrite, resulting in a vermiculated shape [Figure 3A (ii)]. The growth rate of the chiral dendrite toward the achiral crystal was approximately 6  $\mu\text{m/sec}$ . Second, when the chiral dendrites approached and contacted the achiral crystal, as a consequence of the competition between the growth of the chiral dendrite

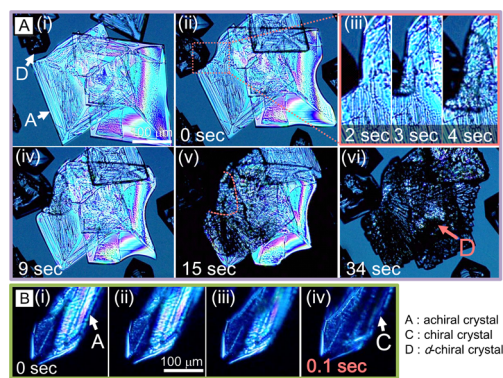


**Figure 3.** In situ polarized-light microscopic images showing two kinds of achiral–chiral polymorphic transformations in solution: (A) the transformation that proceeds with a relatively low transition rate. (i–ii) Micrographs showing the growth of a chiral crystal and dissolution of an achiral crystal. (iii) Micrographs showing a transformation induced by a contact of the achiral crystal with the chiral crystal. (iv–v) Micrographs showing the progress of the phase transition induced by the contact. (vi) A micrograph showing the crystal yielded by the contact-induced phase transition. The chiral crystal exhibits the same chiral sign as the chiral crystal that contacted with the achiral crystal. (B) The transformation that proceeds with a relatively high transition rate. (i–iv) Time-lapse micrographs showing rapid extinction of the achiral crystal.

and the dissolution of the achiral crystal, the achiral crystal immediately began to transform from the point at which the chiral dendrite contacted [Figure 3A (iii)]. The front line of the phase transition advanced radially from the point with a velocity of approximately 35  $\mu\text{m/s}$  [Figure 3A (iv)]. Even after the front line reached the opposite side of the achiral crystal, the bright contrast originating from birefringence remained in some places and gradually darkened [Figure 3A (v)]. After 29 s, a 500  $\mu\text{m}$  parallelogram platy achiral crystal was completely replaced by a chiral crystal [Figure 3A (vi)]. The optical rotation of the contacting chiral dendrites and the transformed one crystal that transformed one indicated that both crystals exhibited the same chiral sign. We observed such contact-induced phase transformation four times, except of that shown in Figure 3A, and confirmed the succession of chirality in all cases.

In addition, rapid transformations as compared to the transition mentioned above were also occasionally observed (see the video, cg500527t\_si\_003.avi, of the Supporting Information). As shown in Figure 3B, the bright contrast due to the birefringence of a 250  $\mu\text{m}$  sized achiral crystal rapidly disappeared within about 0.1 s. The transition rate was approximately 2000  $\mu\text{m/s}$  or more, which was 2 orders of magnitude higher than the other transformations. The rapid phase transition was a rare event compared with the other transformations.

**Observation of Achiral–Chiral Polymorphic Transformation in Air.** We successfully transformed a metastable crystal into a chiral stable crystal by touching the crystal with the tip of a needle (see video, cg500527t\_si\_004.avi, of the Supporting Information). Figure 4 shows a series of micrographs illustrating the transformation triggered by stimulation. From the moment the achiral crystal was stimulated, the bright contrast of the achiral crystal started to change from the fringe of the crystal (Figure 4ii). The change exhibited two steps. First, the interference color, which was homogeneously light

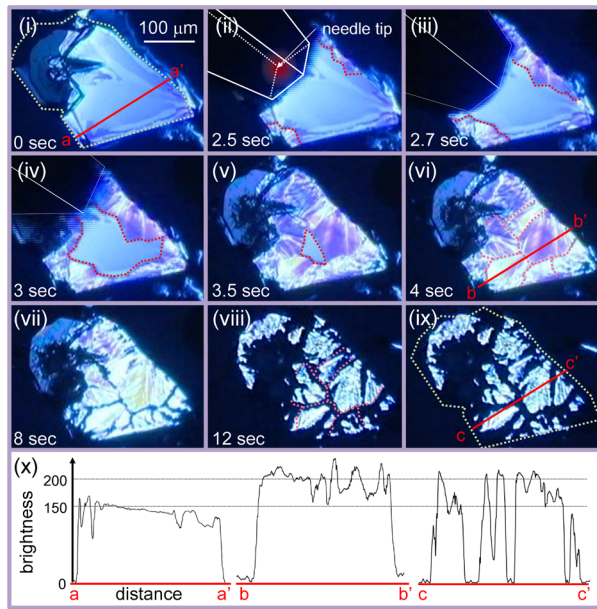


**Figure 4.** In situ polarized light microscopic images showing the solid-state phase transition: (i–ix) Micrographs showing the change in the optical properties of the achiral crystal during the transformation triggered by stimulation using a needle. (i) An achiral crystal before the stimulation. The green dashed line indicates the outline of the achiral crystal [compared to the green dashed line in image (ix)]. The moment when this image was captured is set at 0 s. (ii) The achiral crystal just after stimulation. White lines indicate the outline of the needle used for stimulation, and the circle colored by gradational red indicates the contact point of the needle with the achiral crystal. The red dashed line indicates the front line of the change in optical properties. (vi) The crystal after the first change in optical property. The pink dashed color indicates the boundary of the homogeneous interference color. (x) Brightness distribution profiles for cross lines denoted a-a' in (i), b-b' in (vi), c-c' in (ix), respectively. Brightness of the red color in the RGB histogram was employed for the profile.

blue, began to change into a nonhomogeneous purple color. The purple-based color propagated from several points at the fringe of the crystal toward the center (Figure 4, panels ii–vi). The nonhomogeneity of color appeared to be perpendicular to

the propagation direction (Figure 4v). Figure 4x shows the brightness distribution profiles in the cross lines denoted by a-a', b-b', and c-c'. When comparing the profiles of a-a' and b-b', a considerable difference in brightness can be seen between the crystals before and after stimulation was applied. Specifically, a brightness value before the stimulation was lower than 150, whereas the value after the stimulation was more than 150. When the front lines of the propagation of the purple-based color region collided and overlapped, the overlapped front lines became domain boundaries (Figure 4vi, pink dashed lines). Second, the interference color started to disappear mainly from the domain boundaries and fringe of the crystal (Figure 4, panels vi–viii). The brightness profile in c-c' shows the region whose brightness was close to zero among the region whose brightness was 150–200 (Figure 4x). This observation indicates that the transformation from an achiral crystal to a chiral crystal includes two steps: (1) an optical change during which the brightness value increases and (2) an optical extinction.

## ■ DISCUSSION

**Two Kinds of Phase Transitions: Solid-State and Solution-Mediated.** The phase transitions that occurred in aqueous solution were classified according to their transition rates. While the slower transition progressed at a rate of about  $35 \mu\text{m/sec}$  (Figure 3A), the faster one progressed at a rate of about  $2000 \mu\text{m/sec}$  (Figure 3B). There was a 2 orders of magnitude difference in the transition rates. The large difference probably originated from the difference in the phase transition mechanism. Polymorphic phase transitions during crystallizations from aqueous solutions can be classified into two types: solid-state phase transitions (SSPT) and solution-mediated phase transitions (SMPT).<sup>20</sup> SSPT is caused by structural rearrangements of the atoms and molecules in a metastable structure, that is, SSPT is a diffusion-less transformation. On the other hand, SMPT proceeds by the dissolution of a metastable phase and the recrystallization of a stable phase. Namely, SMPT proceeds by the so-called dissolution/precipitation mechanism, which involves the diffusion of crystal building components. SMPT is diffusion-controlled because the process requires the interchange of the building components between the two phases though the

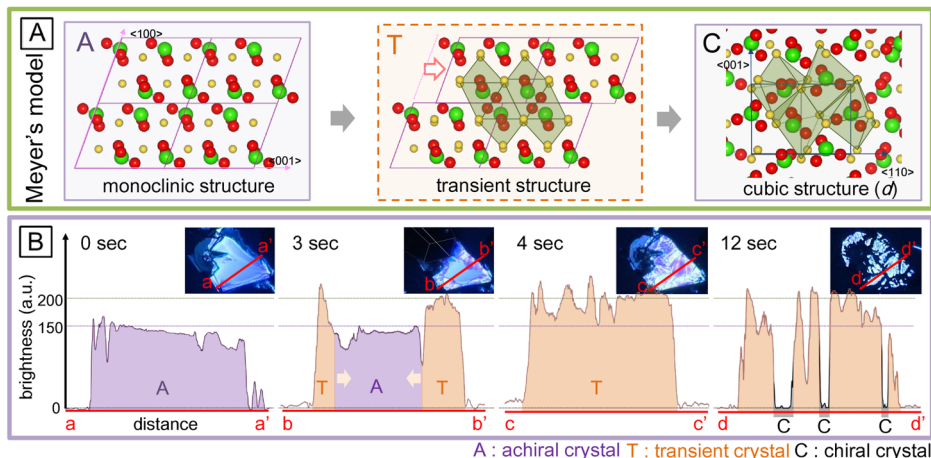


**Figure 5.** Correspondence of optical changes during the solid-state phase transition to Meyer's structural transformation model: (A) Meyer's model describing the structural deformation from phase III, which is a metastable phase in the  $\text{NaClO}_3$  melt growth and is considered to be identical to the achiral phase in solution growth,<sup>18</sup> to a chiral cubic crystal.<sup>21</sup> (B) Change in the brightness profile of crystal with time and correspondence of brightness to structures outlined by Meyer's model. Time indicated in upper left corresponds to time indicated in Figure 4.

solution. The main difference between SSPT and SMPT relates to whether the diffusion of building components is involved or not. Thus, a SSPT transition rate is considered to be faster than that of SMPT. Accordingly, the faster and slower phase transitions in our observation should be classified into SSPT and SMPT, respectively. In the following discussion, we regard the faster transition and the slower transition as SSPT and SMPT, respectively.

**Displacement of Atoms and Determination of Handedness in Solid-State Phase Transitions.** Chirality emerges through structural rearrangements of atoms in the achiral monoclinic structure through the SSPT. Here, we discuss detailed processes of the structural rearrangement by SSPT from the achiral monoclinic structure to the chiral cubic structure. Niinomi et al. pointed out that the achiral metastable monoclinic phase is identical to phase III, which crystallizes when a NaClO<sub>3</sub> melt is cooled down.<sup>18</sup> Besides, Meyer et al. figured out structural displacements explaining the structural deformation from phase III to the chiral cubic phase, and they pointed out that the phase transition is a martensitic transformation (MT).<sup>21</sup> As seen in Figure 5A, the deformation process of Meyer's model is composed of two-step displacements. The first displacement is sliding of the layers that consist of unit cells along the (100) (unique axis *b*) to the direction parallel to the *c* axis by 1/4*c* relative to the adjacent layers. This displacement creates octahedral structures outlined by the sodium atoms. The second displacement is the straining of the octahedral structures. These two deformations describe the structural deformation from phase III to the cubic phase. Since the phase III is identical to the achiral metastable phase, the deformation of SSPT observed in this study is the same as the deformation from the phase III to the cubic phase. Therefore, structural rearrangement during the deformation of SSPT can also follow the model of Meyer et al. Notably, our observation of the achiral crystal exposed to air showed that the transformation undergoes a two-step change in its optical properties (see Results observation of achiral–chiral polymorphic transformation in air). The first optical change was the increase in the brightness. The increased brightness should originate from the optical anisotropy of a noncubic structure, except for the achiral monoclinic phase, implying a transient structure. This transient structure may correspond to the structure after the first displacement in Meyer's model (Figure 5, panels A and B). The solid-state phase transition of the achiral crystal in solution growth may be interpreted by the model.

These considerations above may give rise to a question that lifetime of the transient structure should be extremely short since displacements of atoms should be accomplished instantly. However, in practice, the transient structure remained more than 8 s, indicating that the lifetime was long. The long lifetime can be rationalized by the consideration mentioned below. In the NaClO<sub>3</sub> melt growth, other polymorphs, which are designated as phase II, have been reported as a metastable phase besides the phase III.<sup>22,23</sup> Crystal structure of the phase II still remains undetermined. In accordance with a phase diagram in ref 23 (Figure S1 of the Supporting Information), phase II is the second most unstable phase after the phase III up to 255 °C. Therefore, it is possible that phase II appears as the intermediate phase during the phase transition we observed. On the basis of this idea, we can estimate that the transient structure described in Meyer's model corresponds to the crystal structure of phase II, meaning the transient structure can be not

just a structure required for geometric rationalization but a metastable structure. Therefore, the long lifetime of the transient structure is possibly rationalized by its own metastability.

Meyer's model implies that the transient structure is achiral. This is because the octahedral structures outlined by sodium atoms are chiral, and left-handed and right-handed octahedral structures are alternatively packed in the transient structure. Therefore, the resulting enantiomorph may depend on the direction of the second displacement. The activation energy required to deform the transient structure is expected to be equal for both enantiomorphs. Therefore, SSPT in solution generates the two enantiomorphs in equal probability.

**Dissolution/Growth Controlled Solution-Mediated Phase Transitions and Contact-Facilitated Amplification of Chirality.** SMPT was induced by contact with a chiral crystal. This section discusses the mechanism of contact-induced SMPT. Cardew et al. theoretically classified SMPT according to rate-limiting processes: (1) the dissolution rate of a metastable crystal is higher than the growth rate of a stable crystal (growth-controlled SMPT), or (2) the growth rate is higher than the dissolution rate (dissolution controlled SMPT).<sup>20</sup> The microscopic concentration field around crystals, which governs the growth and dissolution rates, is not taken into consideration in Cardew's theory. Therefore, here, we qualitatively discuss the rate-limiting processes based on a conceivable concentration field surrounding the platy achiral crystal. SMPT proceeds under undersaturated concentrations with respect to the metastable phase<sup>20</sup> (i.e., the achiral crystal dissolves during SMPT). Therefore, the concentration field around the dissolving crystal must be considered. In accordance to the analysis of concentration distribution using interferometric techniques, the concentration distribution around the dissolving crystal increases nonlinearly as it reaches the surface.<sup>24</sup> Thus, we consider the concentration distribution around a dissolving metastable crystal with the following assumptions: (1) the concentration far from the surface of the achiral crystal is slightly supersaturated with respect to the chiral phase; (2) the concentration increases nonlinearly as it reaches the surface; (3) the concentration in the immediate vicinity of the surface is saturated with respect to the metastable achiral phase (Figure 6). For simplicity, the concentration field is assumed to be not influenced by any changes of circumstance (e.g., fluid flow or concentration field originating from other crystals). On the basis of the above assumptions, we discuss three situations: the growth front of a chiral crystal is located (i) significantly far from the surface of the achiral crystal, (ii) at a specific position between (i) and (iii), or (iii) in the immediate vicinity of the surface.

First, let us consider situation (i); namely, before the contact between the chiral crystal and the achiral crystal (Figure 6i). In this situation, the growth front of the chiral crystal is located at the region whose concentration is near equilibrium, causing a slow growth rate of the chiral crystal. The growth rate should be relatively slower than the dissolution rate of the achiral crystal, meaning that this situation is an example of growth-controlled SMPT. In practice, the growth of the chiral crystal would consume the solute dissolved in the surrounding solution and decrease the concentration. Consequentially, the relatively lower concentration would be compensated by dissolution of the achiral crystal, resulting in the vermiculated shape of the achiral crystal reflecting the concentration field surrounding the chiral crystal. For this reason, the dissolution of

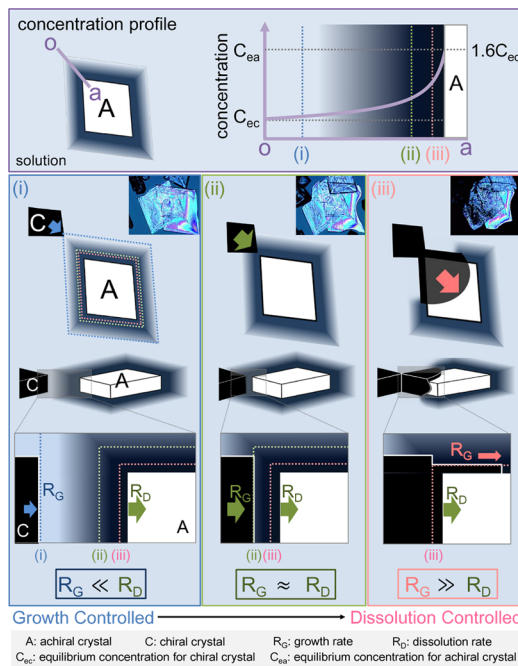


**Figure 6.** Schematic drawing of the mechanism of “contact”-induced solution-mediated phase transition (SMPT). Upper schematic shows the concentration distribution surrounding the achiral crystal. Three drawings denoted by (i), (ii), and (iii) indicate the correlation between the distance between two crystals and consequent relationship of a rate of growth/dissolution. Micrographs appended in the upper left of illustrations (i), (ii), and (iii) are micrographs (i), (ii), and (v) in Figure 3. Situations (i), (ii), and (iii) possibly correspond to before “contact”, at “contact”, and after “contact”, respectively.

the achiral platy crystal, which can be seen in Figure 3, panels (i–ii), is probably a consequence of growth-controlled SMPT.

Second, when the growth front moves to the region closer to the surface of the achiral crystal, the growth rate should eventually become equal to the dissolution rate at a certain position. This position represents situation (ii) (Figure 6ii). The transition from growth-controlled SMPT to dissolution-controlled SMPT occurs at this position. As will be discussed later, situation (ii) represents the moment when the chiral crystal “contacts” the achiral crystal. Note that “contact” does not mean a physical contact, but the irruption of the growth front into the concentration region in which the growth rate of the chiral crystal overcomes the dissolution rate of the achiral crystal.

Third, let us consider what happens when the growth front reaches the immediate vicinity of the surface of the achiral crystal [situation (iii)]. In this situation, the growth front of the chiral crystal erupts into the concentration region in which the growth rate overcomes the dissolution rate (Figure 6iii). Since the region is highly supersaturated with respect to the chiral crystal up to 60% supersaturation,<sup>19</sup> the supersaturation of the region allows the growth rate of the chiral crystal to be remarkably high. It should be emphasized that this region should be very thin. Therefore, the high growth rate occurs exclusively within the thin region. The high growth rate proceeds preferentially along the thin region, causing lateral growth over the surface of the achiral crystal (Figure 6iii). Thus, dissolution-controlled SMPT occurs in this situation. The above-mentioned process for SMPT is supported by two observational evidence: (1) the bright contrast originating from

the achiral crystal remained even after the front line of the transformation crossed the achiral crystal, and (2) the chiral sign of the resulting crystal was certainly the same as the sign of the chiral crystal that contacted the achiral crystal. Therefore, we concluded that the observation in the contact-induced phase transition could be interpreted by the transition from growth-controlled SMPT to dissolution-controlled SMPT due to the “contact”. Hereafter, we will refer to contact-induced SMPT as contact-facilitated SMPT. Even after the chiral crystal covers the entire surface of the achiral crystal, a very thin layer may exist between the chiral crystal and the achiral crystal and might mediate the interchange of building components as proposed by Boerrigter et al. (Figure S2 of the Supporting Information).<sup>25</sup>

A significant aspect of the contact-facilitated SMPT in the chiral symmetry breaking is the inheritance of chirality. In contrast with MT, the resulting enantiomorph generated through contact-facilitated SMPT is strongly directed by the handedness of the crystal that “contacted”, meaning that chirality is amplified when achiral crystals “contact”.

**Determining the Handedness of Chiral Crystals: Preferential and Random Determination Depending on the Two Transitions.** After the nucleation of the achiral monoclinic crystal, the crystal can follow one of two pathways: (1) martensitic transformation (MT) and (2) contact-facilitated SMPT (Figure 7). When the achiral crystal is isolated from

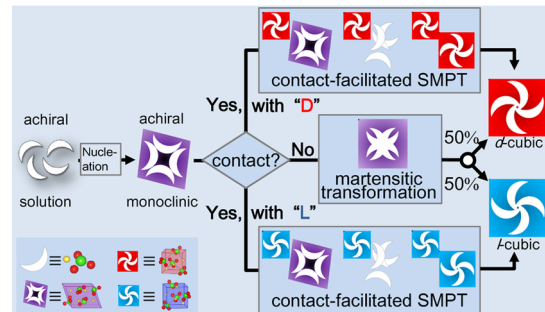


**Figure 7.** Schematic illustration showing the formation pathways for NaClO<sub>3</sub> chiral crystals in aqueous solution via achiral crystals.

chiral crystals, the achiral crystal transforms perhaps through MT. The MT generates both enantiomorphs in equal probability. On the other hand, when the achiral crystal is not isolated from a chiral crystal and “contacts” a chiral crystal, the achiral crystal transforms through contact-facilitated SMPT. The contact-facilitated SMPT preferentially yields the same enantiomorphs as the enantiomorph that contacted the achiral crystal. Therefore, the determination of the enantiomorphs depends on the pathway.

The entire process of crystallization seen in our observation (Figure 2) can be interpreted by a combination of MT and contact-facilitated SMPT. The achiral dendrites initially appeared in a droplet and microscopically transformed to a chiral cubic crystal through MT. The MT might be induced by an increase in the internal energy of the achiral crystal due to the introduction of dislocations accompanying the growth. Subsequently, the chiral phase spreads among the achiral dendrites by contact-facilitated SMPT. MT should hardly occur while the SMPT proceeds because MT is a rare event. Eventually, the chiral crystal generated by MT overwhelms the achiral dendrites by the contact-facilitated SMPT. Namely, the

small imbalance of chirality originating from MT was amplified through contact-facilitated SMPT, and finally a single chirality occupies the entire crystal. MT and contact-facilitated SMPT played a role in the spontaneous emergence of chirality and amplification of chirality, respectively. The chiral symmetry breaking in the crystallization from highly supersaturated solution<sup>3–6</sup> may be interpreted by a similar scenario to that described above (Figure S3 of the Supporting Information).

## CONCLUSIONS

We have examined the achiral–chiral polymorphic transformation, which takes place during the early stages of the NaClO<sub>3</sub> chiral crystallization from highly supersaturated aqueous solution by *in situ* microscopic observations using polarized light microscopy. The observation revealed that an achiral metastable crystal transformed to a stable chiral crystal through one of two different polymorphic transformations: a martensitic transformation (MT) or a contact-facilitated solution-mediated phase transformation (contact-facilitated SMPT). The contact-facilitated SMPT took place when a chiral crystal contacted an achiral crystal. It should be emphasized that the enantiomorph generated by contact-facilitated SMPT was certainly the same as the enantiomorphs that contacted the achiral crystal. Namely, the handedness of the crystal was inherited and amplified through contact-facilitated SMPT. In contrast, MT generated both enantiomorphs in equal probability. Conventionally, the emergence and amplification of chirality are considered to be due to the primary nucleation of chiral crystals and fragmentation, respectively. In contrast, our results demonstrated that MT and contact-facilitated SMPT play important roles in the emergence and amplification of chirality in crystallization from highly supersaturated solutions.

## ASSOCIATED CONTENT

### Supporting Information

Videos showing the *in situ* polarized-light microscopic observations of achiral–chiral polymorphic transformations (cg500527t\_si\_002.avi, cg500527t\_si\_003.avi, and cg500527t\_si\_004.avi). In addition, the phase diagram of NaClO<sub>3</sub> melt growth (Figure S1), the illustrations that explain the mechanism of contact-facilitated SMPT even after a chiral crystal grew over the surface of an achiral crystal (Figure S2), and the illustrations indicating the process of chiral symmetry breaking based on achiral–chiral polymorphic transformations (Figure S3). This material is available free of charge via the Internet at <http://pubs.acs.org>.

## AUTHOR INFORMATION

### Corresponding Author

\*E-mail: niinomi@sic.numse.nagoya-u.ac.jp. Tel: +81-052-789-3249. Fax: +81-052-789-3248.

### Present Addresses

<sup>†</sup>Y.K.: Institute of Low Temperature Science, Hokkaido University, Kita-19, Nishi-8, Kita-ku, Sapporo, Hokkaido 060-0819, Japan.

<sup>‡</sup>H.K.: Faculty of Science and Engineering, Ritsumeikan University, 1-1-1 Nojihigashi, Kusatsu, Shiga, 525-8577, Japan.

### Author Contributions

The manuscript was written through contributions of all authors. All authors have given approval to the final version of the manuscript.

## Notes

The authors declare no competing financial interest.

## ACKNOWLEDGMENTS

The authors are grateful for the support by Grant-in-Aid for Challenging Exploratory Research. no. 23656005 from the Scientific Research of Ministry of Education, Science, and Culture of Japan.

## ABBREVIATIONS

MT, martensitic transformation; SMPT, solution-mediated phase transformation; SSPT, solid-state phase transitions

## REFERENCES

- (1) Kondepudi, D. K.; Kaufman, R. J.; Singh, N. *Science* **1990**, *250*, 975–976.
- (2) Song, Y.; Chen, W.; Chen, X. *Cryst. Growth. Des.* **2008**, *8*, 1448–1450.
- (3) El-Hachemi, Z.; Crusats, J.; Ribó, J. M.; Veintemillas-Verdaguer, S. *Cryst. Growth Des.* **2009**, *9*, 4802–4806.
- (4) El-Hachemi, Z.; Crusats, J.; Ribó, J. M.; Veintemillas-Verdaguer, S. *Angew. Chem., Int. Ed.* **2011**, *50*, 2359–2363.
- (5) Viedma, C. *J. Cryst. Growth* **2004**, *261*, 118–121.
- (6) Buhse, T.; Durand, D.; Kondepudi, D. K.; Laudadio, J.; Spilker, S. *Phys. Rev. Lett.* **2000**, *84*, 4405–4408.
- (7) Viedma, C.; Cintas, P. *Chem. Commun.* **2011**, *47*, 12786–12788.
- (8) Viedma, C. *Phys. Rev. Lett.* **2005**, *94*, 065504.
- (9) Zacharlasen, W. H. Z. *Kristallografiya* **1929**, *71*, 517–529.
- (10) Kipping, W. S.; Pope, W. J. *J. Chem. Soc., Trans.* **1898**, *73*, 606–617.
- (11) Kondepudi, D. K.; Bullock, K. L.; Digits, J. A.; Hall, J. K.; Miller, J. M. *J. Am. Chem. Soc.* **1993**, *115*, 10211–10216.
- (12) Kondepudi, D. K.; Sabanayagam, C. *Chem. Phys. Lett.* **1994**, *217*, 364–368.
- (13) McBride, J. M.; Carter, R. L. *Angew. Chem., Int. Ed. Engl.* **1991**, *30*, 293–295.
- (14) Martin, B.; Tharrington, A.; Wu, X. *Phys. Rev. Lett.* **1996**, *77*, 2826–2829.
- (15) Qian, R. Y.; Botsaris, G. D. *Chem. Eng. Sci.* **1998**, *53*, 1745–1756.
- (16) Qian, R. Y.; Botsaris, G. D. *Chem. Eng. Sci.* **2004**, *59*, 2841–2852.
- (17) Crusats, J.; Veintemillas-Verdaguer, S.; Ribó, J. M. *Chem.—Eur. J.* **2006**, *12*, 7776–7781.
- (18) Niinomi, H.; Yamazaki, T.; Harada, S.; Ujihara, T.; Miura, H.; Kimura, Y.; Kurabayashi, T.; Uwaha, M.; Tsukamoto, K. *Cryst. Growth Des.* **2013**, *13*, 5188–5192.
- (19) Niinomi, H.; Horio, A.; Harada, S.; Ujihara, T.; Miura, H.; Kimura, Y.; Tsukamoto, K. *J. Cryst. Growth* **2014**, *394*, 106–111.
- (20) Cardew, P. T.; Davey, R. J. *Proc. R. Soc. London, Ser. A* **1985**, *398*, 415–428.
- (21) Meyer, P.; Rimsky, A. *Acta Crystallogr., Sect. A* **1979**, *35*, 871–876.
- (22) Meyer, P. C. R. *Seances Acad. Sci., Ser. C* **1972**, *274*, 843–845.
- (23) Ward, M. R.; Copeland, G. W.; Alexander, A. *J. Chem. Commun.* **2010**, *46*, 7634–7636.
- (24) Duran, L.; Shu, J. Z. *J. Cryst. Growth* **2001**, *223*, 181–188.
- (25) Boerriger, S. X. M.; van den Hoogenhof, C. J. M.; Meekes, H.; Bennema, P.; Vlieg, E. *J. Phys. Chem. B* **2002**, *106*, 4725–4731.